Transport from Late Endosomes to Lysosomes, but Not Sorting of Integral Membrane Proteins in Endosomes, Depends on the Vacuolar Proton Pump

Anton W. M. van Weert,* Kenneth W. Dunn,‡ Hans J. Geuze,* Frederick R. Maxfield,‡ and Willem Stoorvogel*

*Universiteit Utrecht, Faculty of Medicine and Institute of Biomembranes, Department of Cell Biology, 3584 CX Utrecht, The Netherlands; and ‡Departments of Pathology and Physiology, Columbia University, New York 10032

Abstract. Endocytosed proteins are sorted in early endosomes to be recycled to the plasma membrane or transported further into the degradative pathway. We studied the role of endosome acidification on the endocytic trafficking of the transferrin receptor (TfR) as a representative for the recycling pathway, the cation-independent mannose 6-phosphate receptor (MPR) as a prototype for transport to late endosomes, and fluid-phase endocytosed HRP as a marker for transport to lysosomes. Toward this purpose, bafilomycin A1 (Baf), a specific inhibitor of the vacuolar proton pump, was used to inhibit acidification of the vacuolar system. Microspectrofluorometric measurement of the pH of fluorescein-rhodamine–conjugated transferrin (Tf)-containing endocytic compartments in living cells revealed elevated endosomal pH values (pH >7.0) within 2 min after addition of Baf. Although recycling of endocytosed Tf to the plasma membrane continued in the presence of Baf, recycled Tf did not dissociate from its receptor, indicating failure of Fe^{3+} release due to a neutral endosomal pH. In the presence of Baf, the rates of internalization and recycling of Tf were reduced by a factor of 1.40 ± 0.08 and 1.57 ± 0.25, respectively. Consequently, little if any change in TfR expression at the cell surface was measured during Baf treatment. Sorting between endocytosed TfR and MPR was analyzed by the HRP-catalyzed 3,3′-diaminobenzidine cross-linking technique, using transferrin conjugated to HRP to label the endocytic pathway of the TfR. In the absence of Baf, endocytosed surface ^{125}I-labeled MPR was sorted from the TfR pathway starting at 10 min after uptake, reaching a plateau of 40% after 45 min. In the presence of Baf, sorting was initiated after 20 min of uptake, reaching ~40% after 60 min. Transport of fluid-phase endocytosed HRP to late endosomes and lysosomes was measured using cell fractionation and immunogold electron microscopy. Baf did not interfere with transport of HRP to MPR-labeled late endosomes, but nearly completely abrogated transport to cathepsin D–labeled lysosomes. From these results, we conclude that trafficking through early and late endosomes, but not to lysosomes, continued upon inactivation of the vacuolar proton pump.

During receptor-mediated endocytosis, ligand–receptor complexes are internalized and transported via clathrin-coated vesicles to endosomes (for reviews see Van Deurs et al., 1989; Courtoy, 1991). In endosomes, ligands and receptors may dissociate from each other, after which receptors and ligands are transported to their specific destination in the cell. Since endocytosed proteins are transported from endosomes to lysosomes, the *trans*-Golgi network (TGN)[1], or to either apical or basolateral plasma membranes (in polarized cells), extensive protein sorting in endosomes occurs. Although the pathways traveled by many proteins from endosomes to these different destinations have been studied intensively, the molecular events involved in protein sorting in endosomes remain largely unknown.

Many endocytosed ligands dissociate from their receptor because of the acidic environment in endosomes (Mell-

Address all correspondence to Willem Stoorvogel, Universiteit Utrecht, Faculty of Medicine and Institute of Biomembranes, Department of Cell Biology, AZU HO2.314, Heidelberglaan 100, 3584 CX Utrecht, The Netherlands. Tel.: (31)-30-506551. Fax: (31)-30-541797.

1. *Abbreviations used in this paper*: apo-Tf, Fe^{3+}-free transferrin; Baf, bafilomycin A1; F-R-dextran, fluorescein-rhodamine dextran; F-R-Tf, transferrin conjugated with both rhodamine and fluorescein; LDLR, low density lipoprotein receptor; MEMH, MEM containing 20 mM Hepes/NaOH, pH 7.2, lacking bicarbonate; MHC, major histocompatibility complex; MPR, cation-independent mannose 6-phosphate receptor; PQ, primaquine; Tf, transferrin; Tf/HRP, transferrin/horseradish peroxidase conjugate; TfR, transferrin receptor; TGN, *trans*-Golgi network; V-ATPase, vacuolar H^+-ATPase.

man et al., 1986). Endocytosed ligands destined for lysosomes travel through endosomal compartments with decreasing pH values (Maxfield and Yamashiro, 1991). These pH values are maintained by a heteromultimeric protein complex, the vacuolar H^+-ATPase (V-ATPase) (reviewed by Gluck, 1993). The activity of the V-ATPase may be regulated by a variety of means; in early endosomes, a membrane potential generated by Na^+,K^+-ATPase has been proposed to have a regulatory effect on ATP-dependent H^+ transport (Fuchs et al., 1989; Cain et al., 1989). Alternatively, V-ATPase activity may be regulated by disulfide bond formation in subunit A of the complex (Feng and Forgac, 1994), a 35-kD cytosolic activator protein (Zhang et al., 1992*a*), a 6.3-kD cytosolic inhibitor (Zhang et al., 1992*b*), and a cytoplasmic heterodimeric protein complex (Xie et al., 1994). Finally, the 50-kD subunit of the clathrin-assembly protein AP-2 (AP50), is involved in the phosphorylation of the β subunit of the V-ATPase (Myers and Forgac, 1993).

Although the activity of V-ATPase in endosomes may be regulated, and differential pH values in the endocytic tract have been measured, the role of endosomal pH in protein sorting has not been completely elucidated; it is obvious that pH-mediated receptor–ligand dissociation is an absolute requirement for their sorting, but the pH requirements for sorting between different integral membrane proteins in endosomes is not clear. Classically, weak bases (e.g., NH_4Cl, chloroquine, and primaquine [PQ]) and proton ionophores (e.g., monensin and nigericin) have been used to neutralize the pH of endosomes, and study pH requirements for endocytic trafficking of integral membrane proteins (for review, see Mellman et al., 1986). In the presence of these compounds, an accumulation of many integral membrane proteins, such as the asialoglycoprotein receptor (Tycko et al., 1983; Schwartz et al., 1984; Strous et al., 1985; Zijderhand-Bleekemolen et al., 1987), low density lipoprotein receptor [LDLR] (Basu et al., 1981), cation-independent mannose 6-phosphate receptor (MPR) (Gonzalez-Noriega et al., 1980; Tietze et al., 1982; Reaves and Banting, 1994), TfR (Stein and Sussman, 1986; Stoorvogel et al., 1987), and TGN38 (Chapman and Munro, 1994), in endosomes was observed. However, in some studies, continued transport in the presence of these agents was reported; for example, neither weak bases nor monensin blocked Fc-receptor recycling when bound to monovalent ligand (Mellman et al., 1984). Together, these inconsistent data indicate that (some) ionophores and/or weak bases are rather nonspecific drugs that may affect parameters, other than pH, that are important for protein transport through endosomes. This idea is illustrated further by the finding that chloroquine inhibited insulin-induced GLUT4 transport to the plasma membrane independently of its action on endosome pH (Romanek et al., 1993).

Bafilomycin A1 (Baf), a macrolide antibiotic (Werner et al., 1984), was shown to inhibit the V-ATPase specifically, without inhibiting F_1F_0- or E_1E_0-ATPases at concentrations up to 1 μM (Bowman et al., 1988). Inhibition by Baf occurs through binding to the membrane-spanning domain of the enzyme, which results in a conformational change of the catalytic site(s) in the cytosolic domain (Hanada et al., 1990; Zhang et al., 1994). The pH in endosomes, as well as in lysosomes, has been shown to be affected by the presence of Baf (Umata et al., 1990; Yoshimori et al., 1991; Johnson et al., 1993; Clague et al., 1994). Since Baf acts specifically on the V-ATPase, it is a powerful tool to study the role of vacuolar pH in protein trafficking through the endocytic pathway without interference of the side effects induced by proton ionophores and weak bases. The effects of this relatively novel drug on protein sorting in endosomes and transport to lysosomes has not been studied extensively.

In the present study, we used Baf to inhibit the vacuolar proton pump activity, and measured its effect on the trafficking of the TfR and the MPR, two model integral membrane proteins that are sorted after endocytic uptake. We have previously used these marker proteins to measure sorting of integral membrane proteins in endosomes (Stoorvogel et al., 1989). TfR and MPR are, after endocytic uptake, recycled to the plasma membrane and transported to late endosomes, respectively. The TfR is involved in the endocytosis of Fe^{3+}-bound transferrin (Tf) (Dautry-Varsat et al., 1983; Klausner et al., 1983). After uptake, Fe^{3+} is released from Tf in endosomes, due to their acidic nature. Fe^{3+}-free Tf (apo-Tf) remains bound to the TfR and is recycled to the plasma membrane. Subsequently, apo-Tf dissociates from the TfR because of its low affinity for the TfR at the neutral pH of the extracellular space. MPR (Sahagian et al., 1981) mediates transport of newly synthesized lysosomal hydrolases to lysosomes (reviewed by Kornfeld and Mellman, 1989); MPR–ligand complexes are transported from the TGN to endosomes, where dissociation occurs. Subsequently, the lysosomal hydrolases are routed to lysosomes, whereas MPR is transported back to the TGN. However, ~10% of the MPR population is present at the cell surface of HepG2 cells (Klumperman et al., 1993), as well as of other cell types (Willingham et al., 1983; Braulke et al., 1987; Geuze et al., 1988). At the plasma membrane, MPR may function as a receptor for lysosomal hydrolases as well as for insulin like growth factor II (Morgan et al., 1987; Kiess et al., 1988). MPR pools in the Golgi complex, endosomes, and at the plasma membrane are in equilibrium (von Figura, 1984; Pfeffer, 1987). Our current results show that internalization of TfR, recycling of TfR to the plasma membrane, as well as intracellular sorting between endocytosed TfR and MPR continued, although at slightly reduced rates, in the absence of an active proton pump. In contrast, transport of a fluid-phase marker from late endosomes to lysosomes was nearly completely blocked.

Materials and Methods

Materials

The human hepatoma cell line Hep G2, clone A16 (Knowles et al., 1980; Schwartz and Rup, 1983) was cultured as described earlier (Stoorvogel et al., 1987). Rabbit antiserum raised against human TfR was a gift from Dr. A. L. Schwartz (Washington University, St. Louis, MO). Rabbit antiserum raised against human MPR and rabbit anti–cathepsin D were kindly provided by Dr. K. von Figura (Georg-August University, Göttingen, Germany). HRP (type VI) and rabbit anti-HRP (P 7899) were from Sigma Chemical Co. (St. Louis, MO). The specificity of these antibodies in immunoprecipitation assays on ^{125}I-labeled HepG2 cells has been described previously (Stoorvogel et al., 1989). ^{125}I-labeling of Tf occurred as reported earlier (Stoorvogel et al., 1988). The Tf/HRP conjugate was pre-

pared and analyzed as described previously (Stoorvogel et al., 1988). The conjugate bound specifically and in a saturable manner to the TfR, and its recycling kinetics were identical to that of nonconjugated Tf. Percoll was obtained from Pharmacia Biotech AB (Uppsala, Sweden). Baf was obtained from Dr. K. Altendorf (Osnabrück University, Osnabrück, Germany). Baf was dissolved in DMSO, and stock solutions were kept at −20°C. The precise concentration of Baf was determined as described by Werner et al. (1984).

TfR-recycling Assays

Cell cultures were washed three times and incubated for 30 min at 37°C in MEM containing 20 mM Hepes/NaOH, pH 7.2, lacking bicarbonate (MEMH), to deplete cells of serum Tf. When indicated, the cells were incubated in the presence of Baf or, for the control cells, solvent (0.2% DMSO) for an additional 30 min at 37°C. Then the cells were incubated in MEMH containing 2 μg/ml ^{125}I-Tf for 60 min at 0°C on a rocker platform, after which nonbound ligand was removed by three washes with MEMH at 0°C. Continuing procedures are described in Results.

DAB Cytochemistry

After depleting the cells of serum Tf (see above), the cells were washed once with MEMH, and four times with Dulbecco's PBS containing $CaCl_2$ and $MgCl_2$ (PBS-C) at 0°C. Plasma membrane proteins were ^{125}I-labeled at 0°C for 30 min in 1 ml PBS-C containing 200 μCi $Na^{125}I$, 100 μg glucose, 5 μg glucose oxidase, and 10 μg lactoperoxidase on a rocker platform (Hubbard and Cohn, 1972). The reaction was stopped by washing the cells four times quickly, and once for 5 min with MEMH at 0°C.

DAB cytochemistry was performed principally as described previously (Stoorvogel et al., 1991*a*). Iodinated cells were incubated for 30 min at 0°C on a rocker platform in 1 ml MEMH containing 25 μg/ml Tf/HRP to prebind ligand to TfR at the plasma membrane. Subsequently, the cells were incubated in 2 ml prewarmed medium containing 25 μg/ml Tf/HRP for the indicated times at 37°C in a waterbath. Baf was added from a stock solution in DMSO when indicated. DMSO (0.2%) was added to control cells. Endocytosis was stopped by washing the cells with MEMH at 0°C. Next, the cells were washed three times with PBS containing 1 mM EDTA at 0°C. Cell-surface proteins were removed by incubation in 2 ml PBS, 1 mM EDTA, and 1 mg/ml proteinase K during 60 min at 4°C. Protease activity was stopped by addition of 1 mM PMSF. The detached cells were collected and washed three times with PBS containing 1 mM EDTA and 1 mM PMSF by centrifugation at 150 *g* for 5 min at 4°C. The cells remained intact, as determined by trypan blue exclusion. Cells were resuspended in 2 ml PBS, 1 mM EDTA, 1 mM PMSF, 300 μg/ml DAB, pH 7.2, and split in two equal samples of 1 ml. To one sample, 0.02% H_2O_2 was added. After 60 min at 0°C, the cells were pelleted by centrifugation at 150 *g* for 5 min at 4°C, and lysed in 1 ml PBS containing 1% Triton X-100, 0.1% SDS, 1 mM EDTA, 0.02% NaN_3, 1 mM PMSF, 0.1 μM leupeptin, and 0.1 μM pepstatin A for 15 min at 0°C. Nuclei were removed from the lysate by centrifugation. ^{125}I-TfR and ^{125}I-MPR were separately immunoprecipitated from samples of the lysate, and analyzed by SDS-PAGE as described previously (Stoorvogel et al., 1987). The gels were scanned and quantified by using a PhosphorImager (Molecular Dynamics, Inc., Sunnyvale, CA). For each time point, ^{125}I-labeled receptor recovered from the sample containing H_2O_2 was expressed as a percentage from the sample lacking H_2O_2. Since both samples were taken from the same pool, heterogeneity in cell numbers after the proteinase K treatment did not contribute to these numbers.

Percoll Density Gradient Fractionation

Cells depleted of serum Tf (see above) were incubated in the presence of either 25 μg/ml Tf/HRP, or 5 mg/ml HRP at 37°C in the presence or absence of 1 μM Baf. Surface Tf/HRP was removed at 0°C using the procedure described in the Results section. Extracellular HRP was removed by extensive washing for 10 min with MEMH at 0°C followed by a chase at 37°C. The chase was required for effective removal of extracellular HRP. Labeled cells were washed sequentially with MEMH and homogenization buffer (HB; 0.25 M sucrose, 10 mM Hepes, pH 7.4) at 0°C. The cells were scraped in 500 μl HB, and homogenized by passage through a 23-gauge needle mounted on a syringe (10 strokes). Nuclei were removed by centrifugation for 1 min at 6,000 rpm in an Eppendorf centrifuge, and 400 μl of the postnuclear supernatant was layered on top of a 7.4 ml Percoll solution (30% Percoll, 0.25 M sucrose, 2 mM $CaCl_2$, 10 mM Hepes, pH 7.4). Gradients were formed by centrifugation for 25 min at 32,000 rpm in an ultracentrifuge (Beckman Instruments, Inc., Fullerton, CA) using a Ti50 rotor (Beckman Instruments, Inc.). Fractions were collected from the bottom of the tube. HRP activity was measured in a spectrophotometer (λ=450 nm) in 0.4 mM *o*-dianisidine, 0.15% Triton X-100, 0.03% H_2O_2 and 50 mM imidazole, pH 6.0.

MPR Detection by Immunoblotting

Cells collected from 6-cm dishes were fractionated as described above. Samples of each fraction were loaded on a 6% SDS-PAGE gel, and analyzed by Western blotting (Stoorvogel et al., 1989). MPR was quantitated using a PhosphorImager®.

Endosome pH Measurement

Human Tf (Boehringer Mannheim Biochemicals, Mannheim, Germany) was iron loaded and Sephacryl S-300 gel (Sigma Chemical Co.) was purified as described previously (Yamashiro et al., 1984). Tf conjugated with both rhodamine and fluorescein (F-R-Tf) was prepared by reacting Tf with succinimidyl esters of both carboxytetramethylrhodamine, and carboxyfluorescein according to the manufacturer's instructions (Molecular Probes, Inc., Eugene, OR) in a ratio of Tf/CF/TMR (8 mg:0.7 mg:0.22 mg). Cellular uptake of F-R-Tf was inhibited in the presence of excess unlabeled Tf, indicating that endocytosis of this conjugate is receptor mediated. Pulse-chase–labeling experiments resulted in loss of detectable label, demonstrating that F-R-Tf is recycled efficiently by cells.

F-R-dextran was prepared by reacting 70,000-mol wt amino dextran (Molecular Probes, Inc.) with succinimidyl esters of both carboxytetramethylrhodamine and carboxyfluorescein according to the manufacturer's instructions (Molecular Probes, Inc.) in a ratio of amino dextran/CF/TMR (10 mg:0.75 mg:0.25 mg).

The confocal microscopic endosome pH assay (Johnson et al., 1993; Dunn et al., 1994) is based on using the ratio of pH-sensitive fluorescein to pH-insensitive rhodamine fluorescence emissions as an indicator of individual endosome pH.

For studies of the pH of Tf-containing endosomes, HepG2 cells, grown in αMEM supplemented with sodium bicarbonate and 8% FCS, were plated onto coverslip-bottomed dishes 2 d before experiments. Dishes were rinsed in medium 1 (150 mM NaCl, 20 mM Hepes, pH 7.4, 1 mM $CaCl_2$, 5 mM KCl, 1 mM $MgCl_2$, 2 mg/ml ovalbumin, and 10 mM glucose), and incubated for 15 min at 37°C. Cells were then incubated with 20 μg/ml F-R-Tf in medium 1 for 30 min on ice. At the end of this period, the incubation medium was replaced with 20 μg/ml F-R-Tf in medium 1 ± 1 μM Baf warmed to 37°C, and dishes were transferred to the stage of an Axiovert microscope (×63, NA 1.4 objective; Carl Zeiss, Inc., Thornwood, NY) maintained at 37°C with an air curtain. Confocal images of cells were obtained in the presence of extracellular F-R-Tf within 2 min of warming to 37°C using an argon laser–scanning confocal attachment (MRC-600; Bio-Rad Laboratories, Richmond, CA). The standard dual-emission configuration of the MRC-600 confocal scanner was modified to increase the detectability of dimly fluorescent endosomes, and to optimize the method's sensitivity to pH differences. In this configuration, 488-nm light is used to stimulate both fluorescein and rhodamine fluorescence. Fluorescein emissions are selected using a 515–545-nm band-pass emission filter, and rhodamine emissions are selected using a 578–633-nm band-pass emission filter (both from Omega Optical Inc., Brattleboro, VT). Light was collected in the two imaging detectors (Bio-Rad) simultaneously. Previous studies have demonstrated that the confocal detection system effectively eliminates the out-of-focus fluorescence of F-R-Tf in the medium from images of cells imaged in the presence of extracellular F-R-Tf. Using image processing techniques developed previously (Maxfield and Dunn, 1990), endosome fluorescence was quantified and the ratio of red to green fluorescence was calculated for each individual endosome. Endosome pH values are estimated from individual endosome fluorescence ratios using calibration curves generated for each experiment using a parallel series of F-R-Tf–labeled cells that are fixed and equilibrated with a range of pH buffers.

Studies of the pH of dextran-labeled endosomes were conducted as described above, except that dishes were incubated in medium 1 for 15 min at 37°C, then incubated on ice for 30 min. At the end of this period, dishes were warmed to 37°C in the presence of 5 mg/ml F-R-dextran ± 1 μM Baf in medium 1 for 30 min. Dishes were then incubated in the absence of F-R-dextran in medium 1 ± 1 μM Baf for 5 min, transferred to the microscope stage, and fluorescence images were collected as described above.

Electron Microscopy

After serum depletion (see above), cells were incubated for 2 h at 37°C in

MEMH containing 20 mg/ml HRP in the presence or absence of 1 μM Baf. After extensive washing with MEMH at 0°C, the cells were fixed for 2 h in 2% paraformaldehyde/0.2% glutaraldehyde in 0.1 M sodium phosphate buffer, pH 7.4. Ultrathin cryosections were processed as described (Harding and Geuze, 1992). Double immunolabeling with 10 and 15 nm protein A–conjugated colloidal gold was performed as described previously (Slot et al., 1991). For quantitation, late endosomes were defined as multivesicular vacuoles containing two or more gold particles labeling MPR. Late endosomes labeled for two or more gold particles representing HRP were considered HRP-positive. Both late endosomes (MPR-positive) and lysosomes (MPR-negative) labeled for cathepsin D. Arbitrarily, lysosomes were identified as vacuoles containing ≥10 gold particles representing cathepsin D. Lysosomes labeled for two or more gold particles representing HRP were scored as being HRP positive. Cryosections were labeled first for HRP, and then for MPR or cathepsin D. For each labeling, three grids, each containing at least 20 cell profiles, were examined.

Results

Baf Interferes with the Release of TfR-bound ^{125}I-Tf

After endocytic uptake, Fe^{3+} dissociates from Tf due to a relatively low endosomal pH. After recycling to the plasma membrane, apo-Tf dissociates from its receptor. Effective inhibition of the endosomal proton pump would prevent dissociation of Fe^{3+}, and consequently inhibit Tf release from recycling TfR. To measure the effect of Baf on the Tf cycle, we first incubated HepG2 cells at 0°C in the presence of ^{125}I-Tf. Nonreceptor bound ^{125}I-Tf was removed, and cells were allowed to internalize ^{125}I-Tf at 37°C after which the release of prebound ^{125}I-Tf at 37°C was measured (Fig. 1). In the absence of Baf, 50% of the prebound ^{125}I-Tf was released into the medium within 10 min, while a near to maximal release was reached after 45 min, consistent with the kinetics of ^{125}I-Tf recycling in HepG2 cells reported previously (Ciechanover et al., 1983; Stoorvogel et al., 1988). As a control, ^{125}I-Tf release was measured in the presence of 0.3 mM PQ, a weak base which neutralizes the endosomal pH and blocks the recycling of TfR (Stoorvogel et al., 1987). Under this condition, only 30% of the prebound ^{125}I-Tf was released after 45 min. Baf inhibited the release of ^{125}I-Tf in a concentration-dependent manner. At 0.1 μM Baf, the release was slightly reduced, while a 45% reduction of the release was measured at 0.25 μM Baf. A maximal inhibition of ^{125}I-Tf release was achieved in the presence of 1 μM Baf, which in fact was even slightly greater than the inhibition with PQ-treated cells. Inhibition of ^{125}I-Tf release was not reversed upon removal of Baf from the medium (not shown).

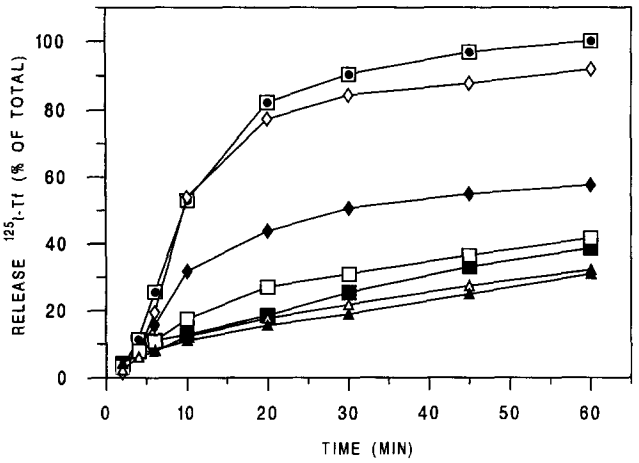

Figure 1. The effect of Baf on ^{125}I-Tf recycling. Cells, cultured in 60-mm dishes, were washed and incubated for 30 min at 37°C in MEMH to deplete receptors of ligand. Surface TfR was labeled at 0°C in the presence of ^{125}I-Tf. Nonbound ligand was removed, and the cells were incubated at 37°C in MEMH (▣), or in MEMH supplemented with either 0.1 μM (◇), 0.25 μM (◆), 0.5 μM (□), 1 μM (△), 3 μM Baf (▲), or 300 μM PQ (■). Release of ^{125}I-Tf was measured from samples taken from the release medium at the indicated time points. Release of nonspecifically bound ^{125}I-Tf was measured from parallel dishes loaded with ^{125}I-Tf in the presence of 100-fold excess of nonlabeled Tf (<10% of total binding), and was subtracted from all values. The release of specifically bound ^{125}I-Tf is plotted as a percentage of total TfR-bound ^{125}I-Tf.

Baf Neutralizes the pH of Tf-containing Endosomes

To measure the effect of Baf on the pH of individual Tf-containing endosomes directly, we incubated HepG2 cells in the continuous presence of F-R-Tf. The cells were imaged as quickly as technically possible (starting at about 2 min), using a confocal microscope at 37°C, in the continuous presence of F-R-Tf. Rhodamine and fluorescein emission images were collected simultaneously, and the emission ratio for each individual endosome was calculated by digital image processing. The resultant ratios were then converted into pH values using a calibration curve constructed by imaging F-R-Tf–labeled cells which had been fixed and equilibrated with a range of pH buffers (Fig. 2 *A*). After internalization, Tf is delivered to endosomes whose pH rapidly decreases. In Fig. 2 *B* this acidification is depicted as the increase in the median rhodamine-to-fluorescein (*R/F*) ratio with time. Comparison with an in situ calibration curve shows that the median endosome pH decreases to ~5.8 within 5 min of internalization. If internalization is conducted in the presence of 1 μM Baf, however, this acidification is completely blocked, with endosomes maintaining a pH >7.0. Addition of the weak base methylamine (Fig. 2 *B*) had no additional effect on endosome pH of Baf-treated cells, indicating that Baf effectively inhibited the acidification of F-R-Tf–containing endosomes. Since transferrin is rapidly sorted into recycling compartments of HepG2 cells, with a $t_{1/2}$ of ~2 min (Stoorvogel et al., 1987), much of the alkalinization induced by Baf at later time points may reflect inhibition of V-ATPases located in recycling endosomes. In Fig. 2 *C*, histograms of endosome R/F ratios are shown for fields of cells imaged between 1:50 and 2:33 min of internalization, a time at which most detectable F-R-Tf would be restricted to sorting endosomes. Even at this early time interval, Baf clearly inhibits acidification, with untreated cells showing a median pH of 6.4, and treated cells a median pH >7.0. These results indicate that Baf prevents acidification of all labeled endosomes, including sorting endosomes, under these conditions. These studies have been repeated three times with the same results.

Baf Inhibits Acidification of Sorting Endosomes and Late Endocytic Compartments

To address the effect of Baf on the pH of endosomes other than those heavily labeled with Tf, the pH of sorting endo-

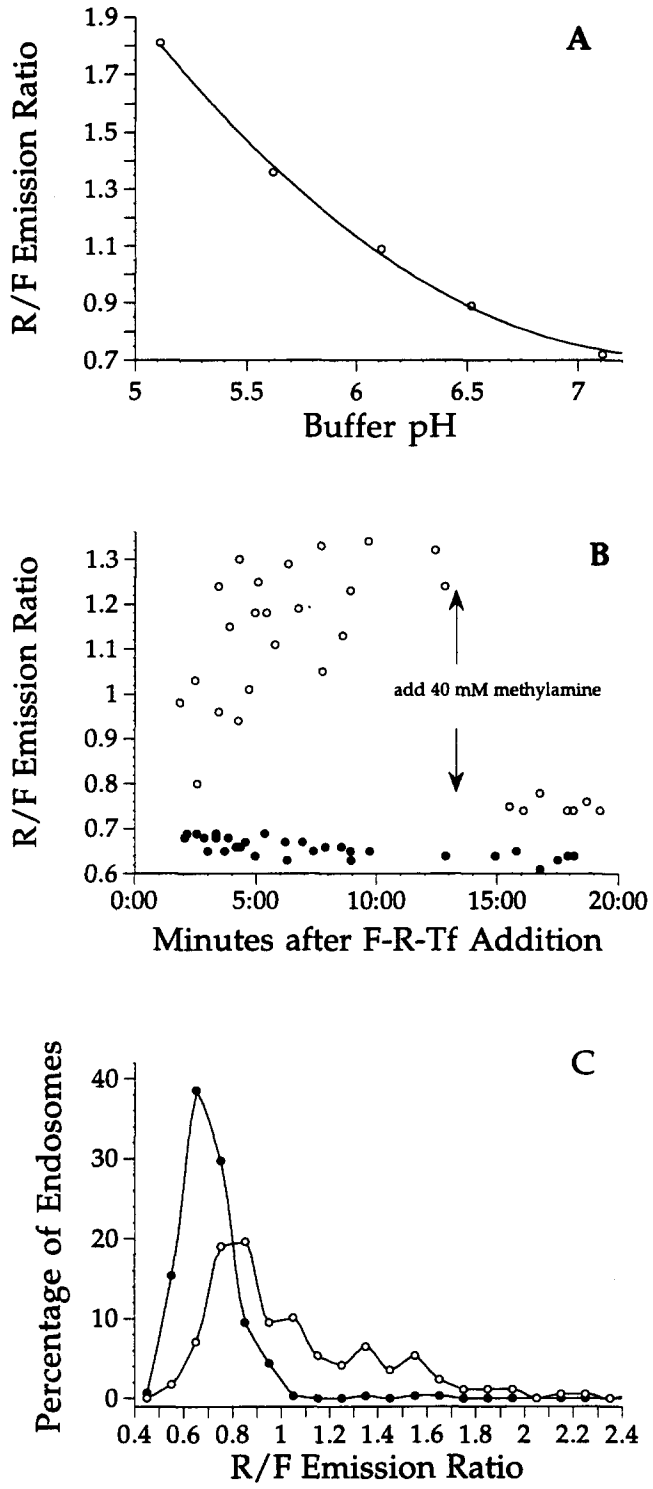

Figure 2. The effect of Baf on the pH of Tf-labeled endosomes. (*A*) Cells were incubated with 20 μg/ml F-R-Tf for 20 min, rinsed, fixed, and equilibrated with pH buffers ranging from pH 5.1 to 7.1. Confocal images were then collected and the rhodamine-to-fluorescein ratio for individual endosomes calculated as described in the Materials and Methods section. The relationship shown here was used as a calibration curve for converting the endosomes R/F ratio into an estimate of endosome pH. The values shown reflect the medians of ~1,000–2,000 endosomes each. (*B*) Fieldwise median endosome pH is shown as a function of time after addition of F-R-Tf (○), or F-R-Tf plus 1 μM Baf (●). (*C*) For control and Baf-treated cells, endosome R/F ratios from three fields apiece, collected between 1:50 and 2:33 after F-R-Tf addition were pooled together into histograms of individual endosome R/F ratios for control cells (○) and Baf-treated cells (●). During this time the median endosome pH of control cells is 6.4, while that of Baf-treated cells is >7.0. These histograms represent R/F measurements from 168 and 272 endosomes from control and Baf-treated cells, respectively.

somes and late endosomes, but not lysosomes (see below), of cells incubated with dextran for 30 min was assayed. The in situ F-R–dextran calibration curve shown in Fig. 3 *A* shows the pH sensitivity of an F-R–dextran conjugate. After 30 min of internalization, dextran is directed to compartments with a median pH of ~5.2 (Fig. 3 *B*). If internalization of dextran is conducted in the presence of 1 μM Baf, however, endosomes are near to neutral, showing a median pH of 6.3. The minor peak occurring at a R/F ratio of 0.45 in the control histogram may result from imaging surface-trapped dextran, or it may represent a population of nonacidic organelles observed in a previous study of HepG2 cells (Tycko et al., 1983). These studies have been repeated four times with the same results.

The Effect of Baf on the Endocytic Cycle of the TfR

Inhibition of the vacuolar proton pump by Baf leads to the inhibition of release of prebound ^{125}I-Tf (Fig. 1). This may be due solely to inhibition of the release of Fe^{3+} from Tf. Alternatively, the recycling of the ^{125}I-Tf/TfR complex to the plasma membrane may have been inhibited as well. Inhibition of TfR/Tf recycling, resulting in a down-regulation of TfR at the plasma membrane by 85%, has been measured in the presence of PQ (Stoorvogel et al., 1987). To discriminate between these two possibilities, we incubated the cells in the presence or absence of 1 μM Baf at 37°C for various periods of time after which the number of specific ^{125}I-Tf–binding sites at the plasma membrane was determined. The number of TfR at the plasma membrane remained constant, irrespective of the presence of Baf (not shown). These results strongly suggest that in the presence of 1 μM Baf the ^{125}I-Tf/TfR complex continued to recycle.

We next studied the effect of Baf on the endocytic uptake and release of ^{125}I-Tf. ^{125}I-Tf was bound to the cells at 0°C. After removing nonbound ^{125}I-Tf, endocytosis of the ^{125}I-Tf/TfR complex was allowed at 37°C in the absence (Fig. 4 *A*) or presence (Fig. 4 *B*) of 1 μM Baf. For every time point, released ^{125}I-Tf, plasma membrane–bound ^{125}I-Tf (as determined by an acidic–neutral wash procedure, see legend), and intracellular ^{125}I-Tf were determined. Irrespective of the presence of Baf, ^{125}I-Tf was rapidly endocytosed. However, in contrast to the control situation (Fig. 4 *A*), Baf prevented a complete depletion of ^{125}I-Tf from the plasma membrane, and a plateau of 20% of the initially bound ^{125}I-Tf remained at the plasma membrane (Fig. 4 *B*). In addition, Baf inhibited the release of ^{125}I-Tf into the medium, and ~60% of the initially bound ^{125}I-Tf was located intracellularly. Since the total number of TfR at the cell surface remained constant, we conclude that the ^{125}I-Tf/TfR complex continuously recycled between endosomes and the plasma membrane in the presence of Baf.

To determine the effect of Baf on the kinetics of inter-

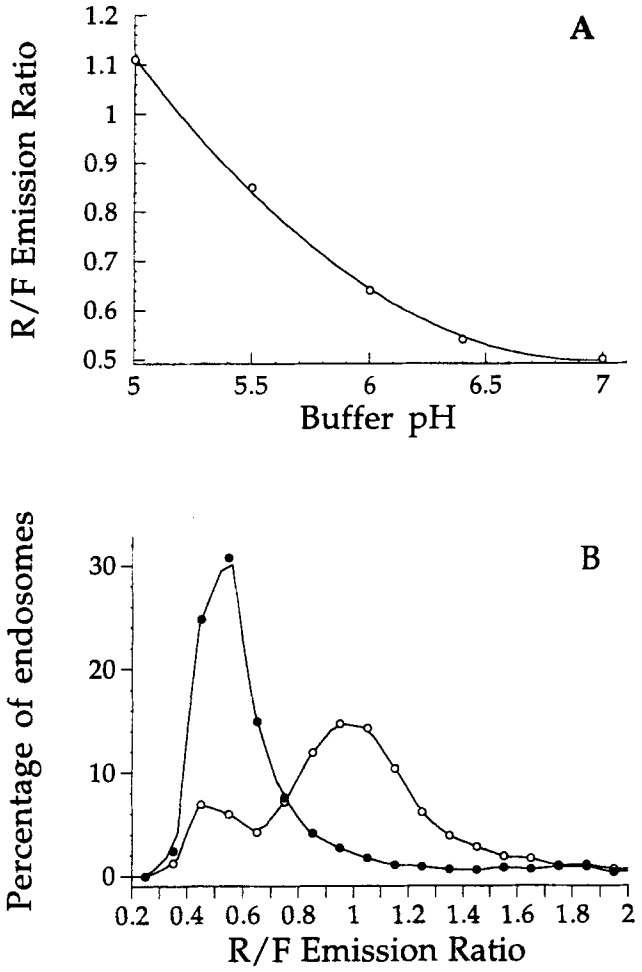

Figure 3. The effect of Baf on the pH of dextran-labeled endosomes/lysosomes. (*A*) Cells were incubated with 5 mg/ml F-R-dextran for 30 min, rinsed, fixed, and equilibrated with pH buffers ranging from pH 5.0 to 7.0. Confocal images were then collected, and the rhodamine-to-fluorescein ratio for individual endosomes calculated as described in the Materials and Methods section. The relationship shown here was used as a calibration curve for converting the endosome R/F ratios of living cells into estimates of endosome pH. The values shown reflect the medians of ~600–1,000 endosomes each. (*B*) Histograms of individual endosome R/F ratios for control cells (○) and for Baf-treated cells (1 μM, ●). Cells were incubated with 5 mg/ml F-R-dextran for 30 min, rinsed into medium 1, and chased for 5 min before image collection. Histograms represent the combined measurements of 1,536 (control cells) and 1,794 (Baf-treated cells) individual endosomes from images collected for up to 20 min, during which time no systematic change in R/F ratio was found. The median R/F ratios for these distributions yield predicted median pH values of 5.2 for control cells and 6.3 for Baf-treated cells.

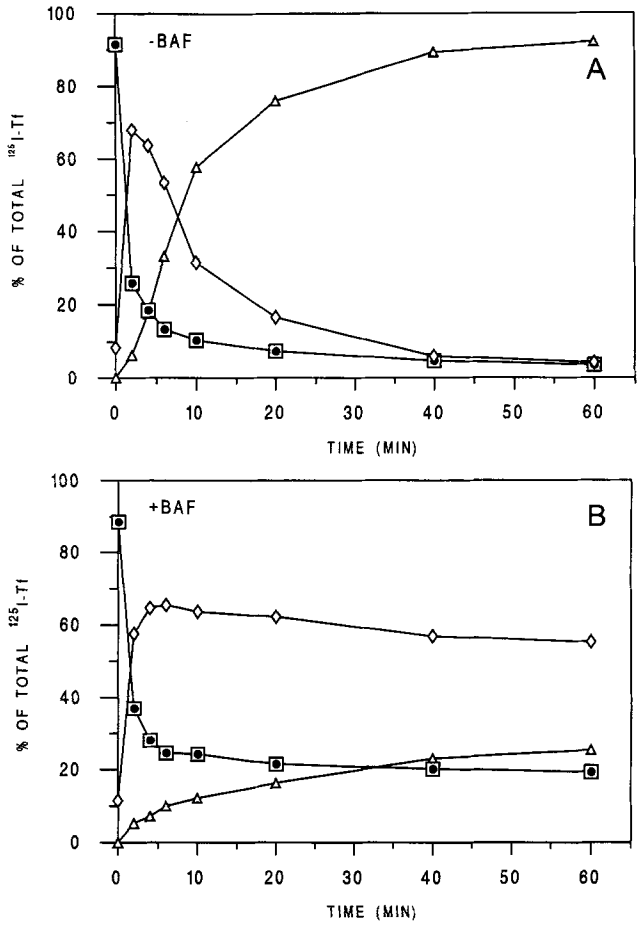

Figure 4. The effect of Baf on the uptake and release of prebound ^{125}I-Tf. Cells were depleted of serum and ^{125}I-Tf was bound to surface TfR as in Fig. 1. Then the cells were incubated for the indicated times at 37°C in MEMH, either in the absence (*A*) or presence (*B*) of 1 μM Baf. Cell surface–bound ^{125}I-Tf was removed from the TfR at 0°C by sequential 10 min incubations at pH 5.0 (25 mM MES, pH 5.0, 150 mM NaCl, 50 μM desferrioxamine) and pH 7.2 (MEMH). Released ^{125}I-Tf (△), ^{125}I-Tf removed by the acidic–neutral wash procedure (▣), and intracellular ^{125}I-Tf (◇) was determined. Nonspecific binding and release of ^{125}I-Tf was determined as in Fig. 1, and was subtracted from all values. Specific ^{125}I-Tf recovered in each sample is plotted as a percentage of total specific ^{125}I-Tf.

nalization exactly, prebound ^{125}I-Tf was allowed to internalize for very short periods of time, to limit recycling to a minimum (Fig. 5). Internalization in the absence or presence of 1 μM Baf occurred with a $t_{1/2}$ of 2.26 ± 0.41 min (n = 3), and 3.15 ± 0.47 min (n = 3), respectively. Although the rates of internalization varied slightly from one experiment to the other, the relative effect of Baf remained remarkably constant; Baf prolonged the internalization time with a factor 1.40 ± 0.08 (n = 3) (Fig. 5, inset). A 30-min preincubation of the cells in the presence of Baf before ^{125}I-Tf binding gave essentially the same result (not shown).

We performed two types of experiments to confirm recycling of ^{125}I-Tf/TfR complex to the plasma membrane in the presence of Baf. Using the first approach, we detected reappearance of diferric ^{125}I-Tf at the plasma membrane in the presence of Baf which could be removed only by sequential washing the cells at 0°C at pH 5 and 7 (not shown). This already indicated directly, although not quantitatively, that recycling of the Tf/TfR complex continued in the presence of Baf. Using a second approach, we determined the rate of recycling of ^{125}I-Tf quantitatively. Cells were labeled with ^{125}I-Tf at 0°C, and after removal of excess of ligand, internalization was allowed for 3 min at 37°C in the presence or absence of Baf or PQ. ^{125}I-Tf remaining at the cell surface was removed by sequential washing of the cells with acidic and neutral media (see leg-

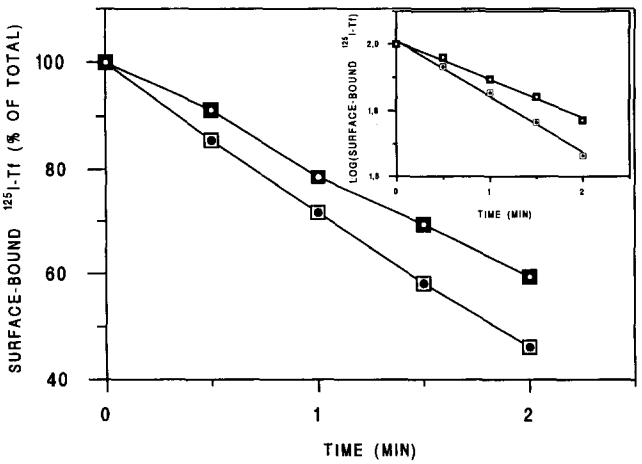

Figure 5. The effect of Baf on the internalization of ^{125}I-Tf. Cells were depleted of serum Tf, and ^{125}I-Tf was bound as in Fig. 1. Subsequently, they were incubated for the indicated times at 37°C in MEMH, either in the absence (▣) or presence (□) of 1 μM Baf. The incubation was stopped by quick immersion of the culture dishes in MEMH at 0°C. Surface-bound ^{125}I-Tf and intracellular ^{125}I-Tf were determined as described in Fig. 4. Nonspecific binding was measured as in Fig. 1, and was subtracted from all values. Specific surface-bound ^{125}I-Tf is plotted as a percentage of total specific ^{125}I-Tf and as the logarithm of the percentage (*inset*). The rate of uptake was calculated using linear regression on the logarithmic plot.

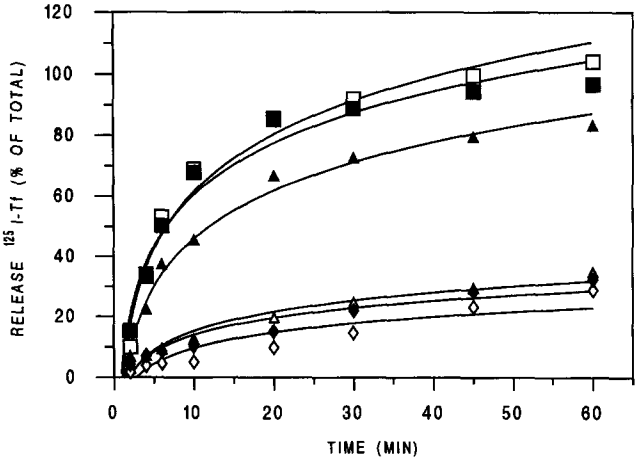

Figure 6. The effect of Baf on the recycling of the ^{125}I-Tf/TfR complex. Cells were depleted of serum and ^{125}I-Tf was bound to surface TfR as in Fig. 1. Uptake was allowed for 3 min at 37°C in MEMH (□, ■), MEMH containing 1 μM Baf (△, ▲), or 300 μM PQ (◇, ◆). ^{125}I-Tf remaining at the cell surface was removed from surface TfR at 0°C by the acidic–neutral wash procedure as described in Fig. 4, using either MES-buffer (*open symbols*) or NaAc/HAc-buffer (*closed symbols*). Incubating cells at 0°C in MES-buffer resulted in the release of Fe^{3+} from transferrin at the plasma membrane only, whereas the NaAc/HAc-buffer resulted in the release of Fe^{3+} from transferrin at the plasma membrane and in endosomes. Then the cells were incubated at 37°C in MEMH in the presence or absence of Baf or PQ, and the release of ^{125}I-Tf was measured from samples taken from the release medium at the indicated time points. Nonspecific ^{125}I-Tf was measured as described in Fig. 1, and subtracted from all values. The release of TfR-bound ^{125}I-Tf is plotted as a percentage of total specifically internalized ^{125}I-Tf, using a logarithmic curve–fitting program.

end, Fig. 4). Two different acidic buffers at pH 5.0 were used, an MES buffer and an NaAc/HAc buffer. Both removed Fe^{3+} from ^{125}I-Tf at the plasma membrane with equal efficiency. In contrast to MES, acetate was capable of penetrating the cells, resulting in acidification of the lumen of endosomes. Consequently, treatment of cells at 0°C with an NaAc/HAc buffer resulted in the dissociation of Fe^{3+} from ^{125}I-Tf in endosomes. Subsequently, the cells were chased at 37°C, and release of ^{125}I-Tf was measured (Fig. 6). NaAc/HAc treatment of the cells did not affect the efficiency of ^{125}I-Tf release in control cells (1.01 ± 0.02, n = 3). PQ efficiently inhibited the release of ^{125}I-Tf in both NaAc/HAc- and MES-treated cells, confirming previous data (Fig. 1; Stoorvogel et al., 1987) which also showed inhibition of ^{125}I-Tf recycling in the presence of PQ. However, when cells are incubated in the presence of Baf, release of ^{125}I-Tf from NaAc/HAc-treated cells, but not from MES-treated cells, was found. Using a logarithmic curve–fitting program, we calculated the $t_{1/2}$ for ^{125}I-Tf release at the different conditions. Release from NaAc/HAc-treated cells occurred with a $t_{1/2}$ of 7.3 ± 0.9 min (n = 3), and 11.3 ± 0.7 min (n = 3) for control cells and Baf-treated cells, respectively. Baf inhibited the release with a factor 1.57 ± 0.25 (n = 3). A 30-min preincubation of the cells in the presence of Baf before ^{125}I-Tf binding gave essentially the same result (not shown). Thus, uptake (Fig. 5) and recycling (Fig. 6) of ^{125}I-Tf were inhibited to about the same extent, resulting in an unchanged number of TfR's at the plasma membrane (not shown).

Sorting of Endocytosed MPR and TfR Continues in the Presence of Baf

After establishing that the uptake and recycling of TfR continued in the presence of Baf, we studied whether sorting from the recycling pathway of an endocytosed integral membrane protein, MPR, was dependent on V-ATPase activity. For this purpose we used DAB cytochemistry on intact cells to measure the degree of colocalization of endocytosed MPR and Tf/HRP in endosomes. The Tf/HRP-catalyzed oxidation of DAB within Tf/HRP-containing endosomes resulted in cross-linking their protein contents to DAB-polymer, rendering it detergent insoluble (Ajioka and Kaplan, 1986, 1987; Geuze et al., 1988; Stoorvogel et al., 1988, 1989, 1991*a*). After cell lysis, immunoprecipitation, and SDS-PAGE, the loss of detectable receptors from samples treated with DAB and H_2O_2 was used as a measure of colocalization with Tf/HRP. To compare the transport pathways of endocytosed MPR with that of TfR, we first surface labeled cells with ^{125}I at 0°C. After endocytosis at 37°C in the continuous presence of Tf/HRP, receptors which remained at, or had recycled to the plasma membrane were removed by proteinase K treatment of the cells at 0°C, leaving only internalized, labeled receptors intact (Stoorvogel et al., 1989). Next, the cells were subjected to DAB cytochemistry, after which ^{125}I-labeled MPR and TfR were immunoprecipitated and quantitated (Fig. 7). After 5 min of uptake, ~85% of both endocytosed ^{125}I-TfR and ^{125}I-MPR were cross-linked after DAB/H_2O_2 incubation, confirming that both receptors colocalized with Tf/HRP (Stoorvogel et al., 1989). Receptor cross-

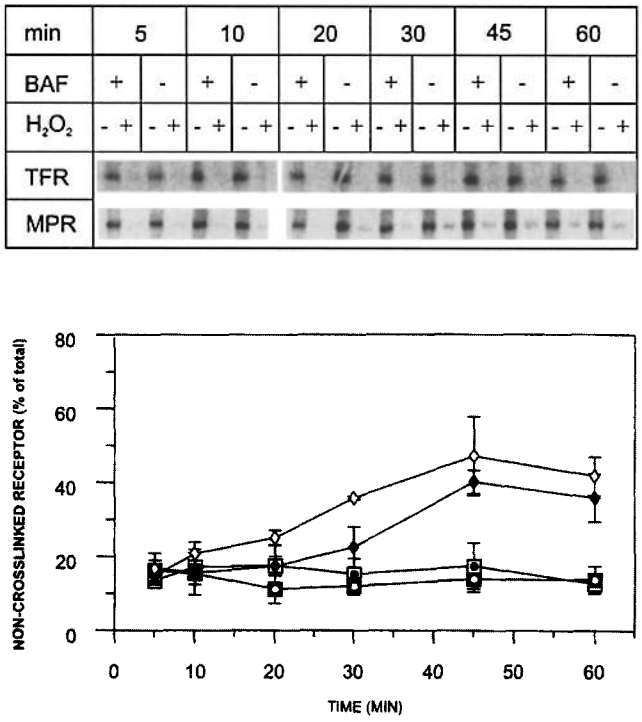

Figure 7. The effect of Baf on sorting of endocytosed MPR and TfR. Cells were depleted of serum Tf as in Fig. 1. Next, the plasma membranes of the cells were ^{125}I-labeled at 0°C. After labeling surface TfR with Tf/HRP for 30 min at 0°C, the cells were incubated at 37°C in MEMH supplemented with Tf/HRP in the absence (−, *open symbols*) or presence (+, *closed symbols*) of 1 μM Baf for the time indicated. Surface-exposed receptors were removed by proteinase-K treatment at 0°C. Samples of the suspended cells were incubated with DAB in the presence (+) or absence (−) of 0.02% H_2O_2. After cell lysis, ^{125}I-MPR and ^{125}I-TfR were immunoprecipitated, and analyzed by SDS-PAGE. Phosphorimages from the gels (top, one representative experiment out of three is shown) were quantitated (bottom, mean values of three experiments ± SD). Non–cross-linked ^{125}I-TfR (▣, ◘) and ^{125}I-MPR (◇, ◆) are expressed as the percentages of total ^{125}I-TfR and ^{125}I-MPR recovered from samples lacking H_2O_2.

linking was dependent on TfR-mediated uptake of Tf/HRP, and did not occur when ^{125}I-labeled receptors and Tf/HRP were localized in different compartments (Stoorvogel et al., 1989). Receptor cross-linking was completely dependent on TfR-mediated uptake of Tf/HRP, since it did not occur when, in addition to Tf/HRP, excess of nonconjugated Tf was present during endocytosis (Stoorvogel et al., 1989). During 60 min of incubation in the continuous presence of Tf/HRP, ~85% of intracellular ^{125}I-TfR remained sensitive to cross-linking, consistent with the idea that Tf/HRP recycled bound to TfR to the plasma membrane. In the absence of Baf, gradual sorting of ^{125}I-MPR from Tf/HRP-containing compartments occurred after 10 min incubation at 37°C, and was completed after 45 min, when ~40% was sorted. In the presence of Baf, an additional delay of ~10 min for sorting of ^{125}I-MPR from the Tf/HRP pathway was observed. However, only a minor effect on the extent of sorting was measured after 45 min. Preincubation of the cells with Baf for 30 min at 37°C before ^{125}I-labeling of the cells gave the same result (not shown). From these results we conclude that, although the onset of sorting was delayed by about 10 min, the principle of sorting between ^{125}I-TfR and ^{125}I-MPR continued independent of proton pump activity.

Baf Inhibits Transport of HRP from Late Endosomes to Lysosomes

The finding that sorting of endocytosed MPR and TfR continued in the presence of Baf suggested that Baf did not affect transport to late endosomes. To confirm this, and study the effect of Baf on transport to lysosomes, trafficking of a fluid-phase endocytic marker, HRP, was examined. HRP (5 mg/ml) was internalized and chased for either 5 min or 2 h in the presence or absence of Baf. The cells were homogenized and fractionated on Percoll density gradients, and HRP activity was determined (Fig. 8). The distribution of endosomes and lysosomes were defined in control experiments. Endocytosed Tf/HRP (early endosomes) and MPR (late endosomes and TGN) peaked in fractions 7–9, whereas lysosomes localized to fractions 2–4 (Fig. 8 *A*). The distribution of HRP did not change when Baf was present during a short period of uptake (5 min pulse, 5 min chase; Fig. 8 *B*). The distribution of Tf/HRP endocytosed for 1 h was also not affected by Baf (not shown). However, when cells were pulsed with HRP for 15 min and chased for 2 h in the presence of Baf, no HRP activity was detected in the lysosomal fractions (Fig. 8 *C*). A redistribution of the lysosomes to endosomal fractions due to Baf could be excluded, since HRP that was transported to lysosomes in the absence of Baf was not redistributed upon a subsequent Baf-treatment of the cells (not shown). We thus conclude that transport from endosomes to lysosomes was inhibited in the presence of Baf. This inhibitory effect was not reversed within 1 h upon removal of Baf from the medium (not shown).

Continued sorting of endocytosed MPR and TfR in the presence of Baf already suggested that transport to late endosomes was not affected (Fig. 7). To confirm this independently, we studied the intracellular distribution of a fluid-phase endocytic marker using immunoelectron microscopy. HRP (20 mg/ml) was endocytosed for 2 h in the presence or absence of Baf. The cells were fixed and processed. After fixation, ultrathin cryosections were prepared and immunogold double-labeled for HRP and MPR (Fig. 9, *A* and *B*) or HRP and cathepsin D (Fig. 9, *C* and *D*). The morphology of MPR-containing late endosomes and cathepsin D–labeled lysosomes did not change notably after Baf treatment. MPR-labeled endosomes and cathepsin D–labeled lysosomes were scored for the presence of HRP (Fig. 10; for quantitation see also the Materials and Methods section). In the absence or presence of Baf, 79.5 ± 16.0% (n = 3) and 75.8 ± 7.3% (n = 3), respectively, of MPR-containing multivesicular bodies/late endosomes were labeled for HRP. Multivesicular bodies/late endosomes labeled for 10.9 ± 4.7 and 4.9 ± 0.8 gold particles per vacuole in the absence and presence of Baf, respectively. A reduction of HRP-labeling in late endosomes after Baf treatment was expected due to a less efficient accumulation of HRP in the presence of Baf (Fig. 8 *C*). We conclude that late endosomes remained fully accessible to endocytosed material in the presence of Baf.

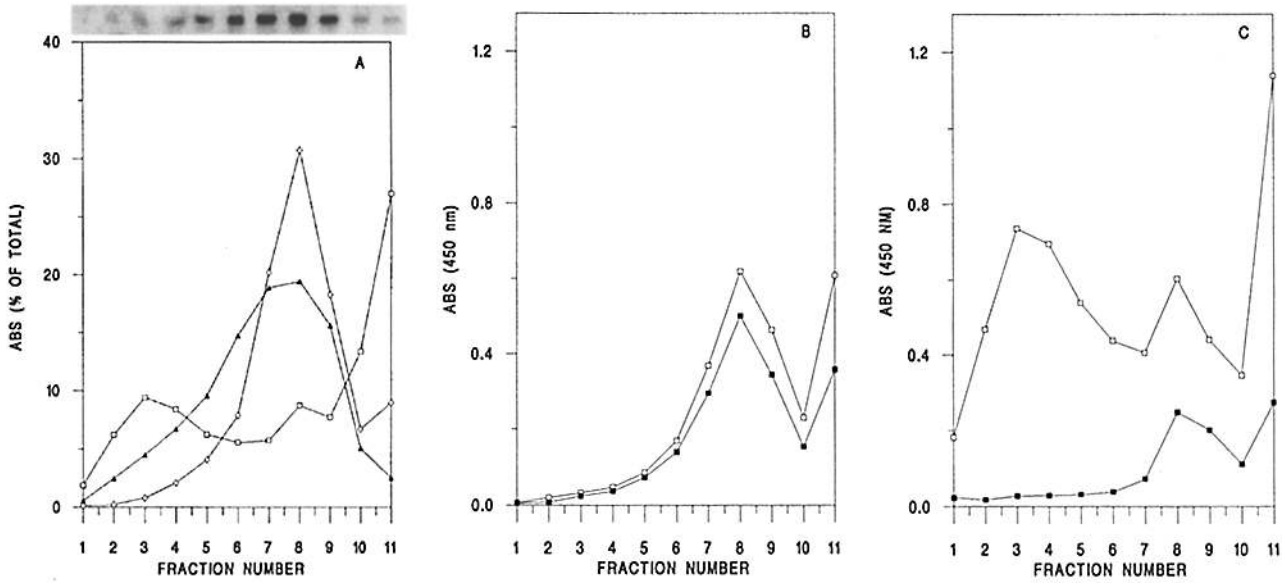

Figure 8. The effect of Baf on transport of endocytosed HRP. Cells were incubated at 37°C in MEMH containing either 25 μg/ml Tf/HRP or 5 mg/ml HRP. After homogenization, cells were fractionated on Percoll density gradients and HRP activity in the fractions was determined and plotted as the percentage of total activity in the gradient (*A*) or absorption at 450 nm (*B*, *C*). The results presented have been corrected for the background absorption obtained using cells that have been incubated in the absence of any marker. (*A*) Early endosomes were defined in cells that had been incubated for 10 min in the presence of Tf/HRP (◇). Surface-bound Tf/HRP was removed at 0°C (see legend, Fig. 4). Late endosomes were defined by detection of MPR. Samples from the density gradient were analyzed by SDS-PAGE and Western blotting (*A*, *top*). The images were quantitated and plotted as percentage of total (▲). Lysosomes were identified in cells that had been incubated for 15 min in the presence of HRP and chased for 2 h in the absence of HRP (□). (*B*) Transport of HRP to early endosomes. Cells were incubated for 5 min in the presence of HRP, and chased for 5 min in the absence of HRP. These incubations were performed either in the absence (□) or presence (■) of 1 μm Baf. (*C*) Transport of HRP to lysosomes. Cells were incubated for 15 min in the presence of HRP and chased for 2 h in the absence of HRP. These incubations were performed either in the absence (□) or presence (■) of 1 μm Baf. The experiments have been performed three times, essentially giving the same result.

Both late endosomes and lysosomes contained cathepsin D. Lysosomes were defined as large electron-dense vacuoles labeled for ≥10 cathepsin D molecules. This arbitrary measure almost completely ruled out multivesicular MPR-labeled late endosomes. Using this definition, lysosomes labeled for 27–38 gold particles on average, irrespective of the presence of Baf. In the absence or presence of Baf, 84.4 ± 2.7% (n = 3) and 15.6 ± 2.7% (n = 3), respectively, of cathepsin D–containing lysosomes were labeled for HRP (Fig. 10). Lysosomes labeled for 15.1 ± 2.4 and 0.9 ± 0.2 gold particles per vacuole in the absence and presence of Baf, respectively. These data are consistent with those obtained using cell fractionation (Fig. 9 *C*). We conclude that in the presence of Baf, transport into the degradative pathway was blocked at the step from late endosomes to lysosomes.

Discussion

We investigated the requirement of an active vacuolar proton pump for correct targeting to early endosomes, late endosomes, and lysosomes. Toward this goal we used a specific inhibitor of the vacuolar proton pump, Baf. Microspectrofluorometric measurement of the pH of F-R-Tf–containing endocytic compartments revealed that in <2 min after addition of 1 μM Baf pH values increased to >7.0 (Fig. 2). Baf inhibited the release of endocytosed ^{125}I-Tf in a concentration-dependent manner, with a maximal inhibition at 1 μM (Fig. 1). These data are consistent with the idea that pH-mediated Fe^{3+} release from Tf is required for release of Tf from its receptor after recycling to the plasma membrane (Dautry-Varsat et al., 1983; Klausner et al., 1983). Both the microspectrofluorometric data (Figs. 2 and 3) and the recycling data (Figs. 1, 4, and 6) indicate that in the presence of 1 μM Baf, the acidification of Tf-labeled compartments was inhibited. Both in the presence of PQ and Baf, 30% of ^{125}I-Tf was released after 60 min at 37°C. This result is in good agreement with other reports (Octave et al., 1982; Klausner et al., 1983; Ciechanover et al., 1983; Johnson et al., 1993) which show a reduced release of prebound ^{125}I-Tf in the presence of Baf or lysosomotropic agents such as PQ, chloroquine, and ammonium chloride.

Uptake (Fig. 5) and recycling to the plasma membrane (Fig. 6) of ^{125}I-Tf were inhibited in the presence of Baf by a factor of 1.40 ± 0.08 and 1.57 ± 0.25, respectively. Since these factors are not significantly different, no change in expression of TfR at the plasma membrane upon exposure to Baf was detected (not shown). The half-time of internalization in the absence of Baf was 2.26 ± 0.41 min (Fig. 5), which is in agreement with values reported previously for HepG2 cells (Ciechanover et al., 1983). Reports on the effect of inhibitors of the vacuolar proton pump are not consistent (Johnson et al., 1993; Clague et al., 1994; Bénaroch et al., 1995). A decrease in the rate of recycling of TfR in TfR-transfected CHO cells as a consequence of Baf

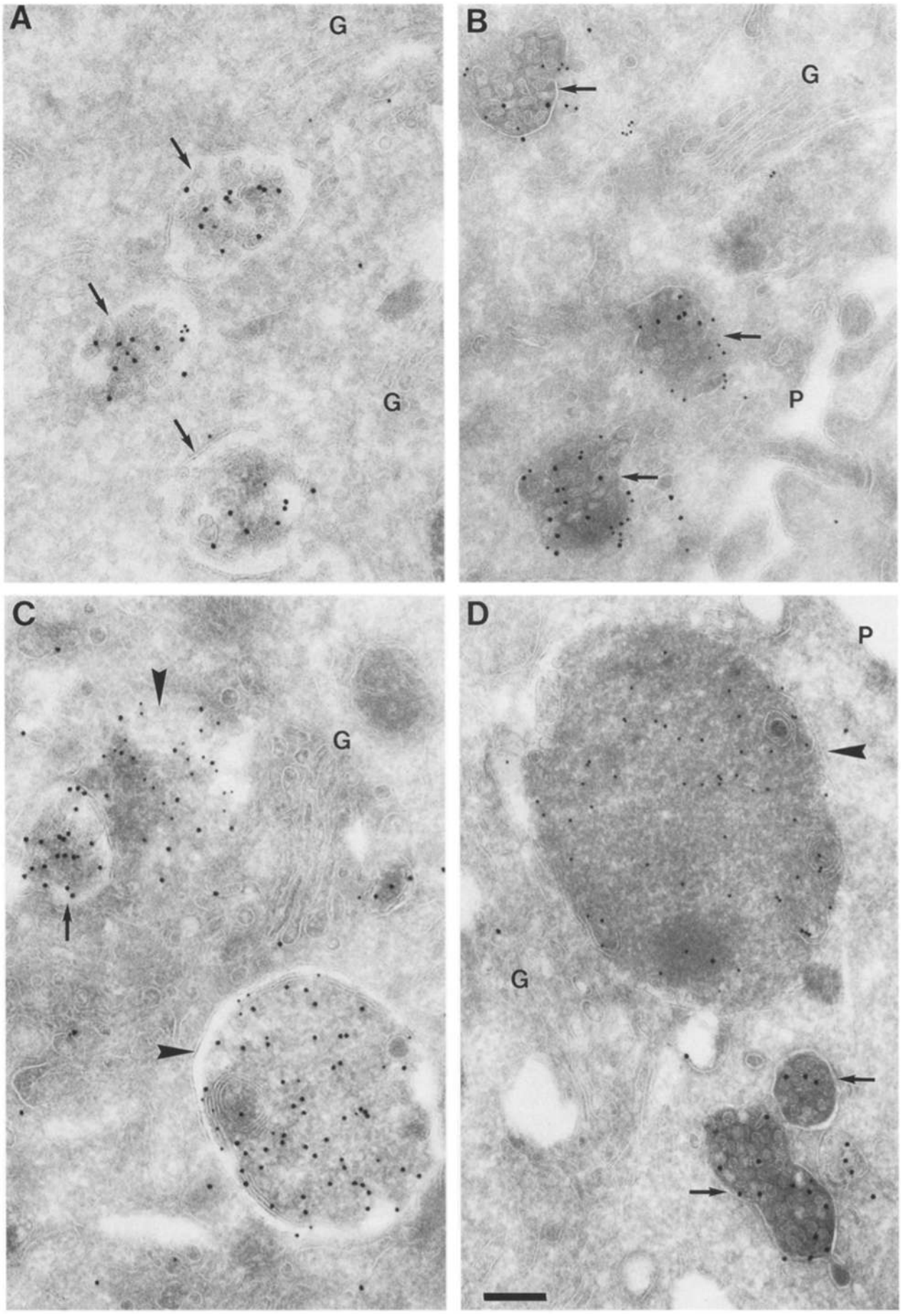
A
G
G
B
G
P
C
G
D
P
G

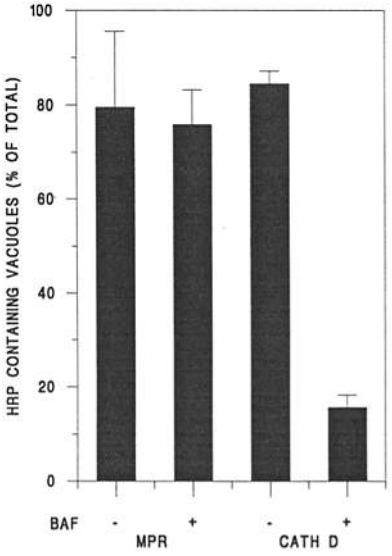

Figure 10. Transport of HRP to late endosomes and lysosomes. Late endosomes (*MPR*) and lysosomes (*cath D*) identified from images as in Fig. 9 were quantitated for the presence of HRP as described in the Results and Materials and Methods sections. Quantitations were performed for three grids at each condition (mean ± SD).

treatment has recently been reported (Johnson et al., 1993). This effect is very similar to that reported here for TfR in HepG2 cells. However, in contrast to our data, TfR internalization in these cells was not affected by Baf. Consequently, it was reported that TfR recycling in CHO cells was specifically slowed in the presence of Baf. In addition, it was shown that the effect of Baf on TfR recycling could largely be eliminated by replacing either of the two aromatic amino acids within the TfR's cytoplasmic YTRF internalization motif. Since we found that for HepG2 cells both uptake and recycling are slowed to the same extent in the presence of Baf, in these cells the number of TfR at the plasma membrane remained constant. The differences in these two studies may be due to differential transport mechanisms of endogenous TfR in HepG2 cells vs. human TfR in CHO cells.

The effects of acidotropic agents (weak bases) or H^+ ionophores on transport to endosomes and lysosomes has been studied extensively, but the results have not been consistent (for a review see Mellman et al., 1986). For example, transport of endocytosed HRP to lysosomes was not inhibited by NH_4Cl in a macrophage cell line (Ukkonen et al., 1986). In the presence of monensin it has been shown that 50% of the LDLR (Basu et al., 1981) and TfR (Stein and Sussman, 1986) were trapped inside the cell (monensin-sensitive pool), whereas the other half of the receptor population continued to recycle (TfR) or remained at the cell surface (LDLR) (monensin-resistant pool). In contrast, PQ and chloroquine treatment resulted in the intracellular accumulation of nearly all ASGPR and TfR (Schwartz et al., 1984; Stoorvogel et al., 1987; Zijderhand-Bleekemolen et al., 1987). MPR was also shown to accumulate intracellularly in the presence of chloroquine (Chapman and Munro, 1994; Reaves and Banting, 1994). Although the rate of both uptake and recycling of the TfR to the plasma membrane are mildly affected by Baf, our data show that acidification of endosomes is not required to complete the endocytic cycle. We therefore conclude that the effects of weak bases and ionophores on the endocytic cycle of the TfR are not a consequence of their neutralizing effect on the endosomal pH. Indeed, chloroquine has been shown to inhibit GLUT4 transport to the plasma membrane independently of its action on endosome pH (Romanek et al., 1993). One possible explanation may be that these drugs also affect the generation of ATP (Strous et al., 1985).

We investigated the effect of inhibition of the vacuolar proton pump by Baf on the sorting between endocytosed MPR and TfR. Previously, we (Stoorvogel et al., 1987, 1988, 1989, 1991*a*; Geuze et al., 1988) and others (Ajioka and Kaplan, 1986, 1987) used DAB cytochemistry on cell fractions to measure protein colocalization with endocytosed HRP-(conjugates). More recently we performed DAB cytochemistry on intact cells to measure protein colocalization (Stoorvogel et al., 1991*a*; Rijnboutt et al., 1992; Strous et al., 1993). Using DAB cytochemistry on intact cells, we found that after endocytic uptake in the continuous presence of Tf/HRP, 85% of ^{125}I-TfR was cross-linked to the DAB polymer due to the peroxidase activity of the Tf/HRP conjugate (Fig. 7), consistent with cross-linking efficiencies reported previously (Stoorvogel et al., 1991*a*). Immediately after uptake, cross-linking of ^{125}I-MPR to DAB polymer occurred with an efficiency of 85% as well. Since the efficiency of cross-linking of MPR in early endosomes is reduced at a concentration of Tf/HRP below 25% of its maximal value (Stoorvogel et al., 1989), and the TfR concentration in late endosomes is low (Stoorvogel et al., 1991*b*), sorting of endocytosed MPR from TfR during the maturation of early to late endosomes resulted in less efficient cross-linking (Fig. 7). After reaching late endosomes, ^{125}I-MPR was expected to shuttle largely between late endosomes and the TGN. Both these compartments contained significant, but low, amounts of endocytosed Tf/HRP (Stoorvogel et al., 1988, 1989, 1991; Rijnboutt et al., 1992; Strous et al., 1993), resulting in inefficient cross-linking of ^{125}I-MPR (Fig. 7). Indeed we detected, although not quantitatively, endocytosed Tf/HRP in late endosomes/multivesicular bodies and in the TGN, independent of the presence of Baf (not

Figure 9. The effect of Baf on transport of HRP to late endosomes and lysosomes. Cells depleted of serum (see legend, Fig. 1) were incubated for 2 h at 37°C in MEMH containing 20 mg/ml HRP, in the absence (*A*, *C*) or presence (*B*, *D*) of 1 μM Baf. Ultrathin cryosections were double-labeled for HRP (15 nm gold) and MPR (10 nm gold) (*A*, *B*) or HRP (15 nm gold) and cathepsin D (10 nm gold) (*C*, *D*). Electron micrographs show multivesicular bodies (➔), lysosomes (➤), Golgi complex (*G*), and plasma membrane (*P*). Multivesicular bodies, identified by the presence ≥2 gold particles representing MPR, were labeled for HRP in the absence (*A*) and presence (*B*) of Baf. Lysosomes, identified by the presence of ≥10 gold particles representing cathepsin D, were labeled for HRP in the absence (*C*) but not in the presence (*D*) of Baf. Bar, 200 nm.

shown). Previously we reported that after endocytic uptake, a significant amount of the fluid-phase marker HRP was also targeted to the TGN (Strous et al., 1993). Transport of HRP to the TGN, identified by the presence of both MPR and the adaptor complex AP1, continued irrespective the presence of Baf (not shown). Together, these results show that transport from the cell surface to endosomes, as well as from endosomes to the TGN, continued after inhibition of the vacuolar proton pump by Baf.

Using DAB cytochemistry on cell fractions, we have previously reported sorting of 70% of endocytosed MPR within 45 min of uptake from Tf/HRP-containing endosomes (Stoorvogel et al., 1989). Our current data, which have been obtained from experiments in which DAB cytochemistry was performed on intact cells (Fig. 7), revealed sorting of 40% of endocytosed MPR from the Tf/HRP pathway within 45 min. These quantitative differences possibly may be explained by the finding that during cell homogenization significant proportions of late endosomes and lysosomes are disrupted (not shown). Consequently, DAB cytochemistry performed on cell homogenates as compared with intact cells resulted in less efficient cross-linking of the total pool of late endosomal proteins. Our current finding that 60% of endocytosed ^{125}I-MPR remained in contact with recycling Tf/HRP is not surprising, since we have previously shown that in HepG2 cells endosomes gradually mature from Tf/HRP-rich/MPR-poor ("early") endosomes to Tf/HRP-poor/MPR-rich ("late") endosomes resulting in a large overlap in the intracellular distributions of TfR and MPR (Stoorvogel et al., 1991*b*, and references therein). In the presence of Baf, a delay of about 10 min as compared with the control for sorting of ^{125}I-MPR from the Tf/HRP pathway was observed. However, only a minor effect on the extent of sorting was measured after 45 min. We conclude that the basic mechanism of sorting between endocytosed TfR and MPR, but not the rate of sorting, is independent of proton pump activity.

In the presence of the microtubule-disrupting drug, Nocodazole, "carrier vesicles", described as transport intermediates between early and late endosomes, have been reported to accumulate (Gruenberg et al., 1989). Recently, Clague et al. (1994) described that in nocodazole-treated BHK cells Baf inhibited the formation of these vesicles, resulting in complete inhibition of transport of endocytosed HRP to late endosomes. These conclusions are inconsistent with our findings. The differences cannot be explained by the suggestion that MPR/HRP-labeled late endosomes in the current study are the equivalent of carrier vesicles, since the formation these vesicles has been reported to be inhibited by Baf (Clague et al., 1994). Using HRP as a fluid-phase marker, we showed that transport to MPR-containing late endosomes continued irrespective of the presence of Baf (Figs. 9 and 10). MPR is a valid marker for late endosomes in Baf-treated cells for the following reasons: (1) In the presence of Baf, endocytosed ^{125}I-MPR was sorted from the TfR pathway (Fig. 7). Tf/HRP was present in the medium during the entire incubation. Thus, ^{125}I-MPR was also segregated from TfR endocytosed at later time points. At these conditions, segregated ^{125}I-MPR was not sequestered in early endosomes inaccessible to newly endocytosed proteins; MPR was transported to endocytic compartments that contained little Tf/HRP, but were filled with the fluid-phase marker HRP (Fig. 9). (2) In the presence of Baf, MPR/HRP-labeled compartments clearly have a late endosomal morphology, they are large and, more important, they are multivesicular. In addition, their subcellular location, proximate to the Golgi region (Fig. 9), corresponds to that of late endosomes. Several arguments can be brought up to explain the apparent discrepancies between our data and the observations of Clague et al. (1994): (1) In HepG2 cells late endosomes derive from early endosomes by maturation, and TfR was detected in early as well as late endosomes (Stoorvogel et al., 1991*b*). (2) The results of Clague et al. (1994) may be due to synergistic effects of nocodazole and Baf. (3) In their study, late endosomes have not been defined by a marker. (4) The effect of Baf on the formation of carrier vesicles was measured at a single time point only (30 min). Our kinetic data show a reduced sorting of endocytosed ^{125}I-MPR and ^{125}I-TfR after 30 min of uptake in the presence of Baf, but a near to complete sorting after 45 min (Fig. 7).

We found that Baf strongly inhibited transport from late endosomes to lysosomes using two independent approaches, cell fractionation (Fig. 8), and immunoelectron microscopy (Figs. 9 and 10). Yoshimori et al. (1991) reported that endocytosed EGF was not degraded, but at least partly recovered in lysosomes in the presence of Baf. However, these authors did not quantitate transport of EGF receptor to lysosomes in the presence of Baf. We found that after 2 h of continuous uptake of HRP, labeling of lysosomes for HRP was reduced 17-fold in the presence of Baf. Thus, although transport was strongly inhibited, it was not completely blocked. Therefore, Yoshimori's data are not necessarily inconsistent with our observations.

Recently, it was found that concanamycin B, a macrolide antibiotic related to Baf which also inhibits the vacuolar proton pump, prevented efficient targeting of endocytosed markers to major histocompatibility complex (MHC) class II–containing compartments (Bénaroch et al., 1995). MHC class II compartments are unique organelles with lysosomal characteristics that are specific for MHC class II–positive antigen-presenting cells (see Bénaroch et al., 1995, and references therein). Bénaroch et al. did not identify the precise site at which transport of MHC class II was inhibited by concanamycin B. To interpret their results, they referred to the block in transport from early to late endosomes reported by Clague et al. (1994). However, their results can be explained equally well by a block in transport from late endosomes to MHC class II compartments. Thus, when MHC class II compartments are connected to the endocytic pathway distal to late endosomes, the findings of Bénaroch et al. (1995) are consistent with our current findings.

We have shown that early endosomal V-ATPase is effectively blocked in the presence of Baf (Fig. 2). However, at the same conditions, the pH of sorting endosomes/late endosomes was not completely neutral in the presence of Baf (Fig. 3). A lysosomal pH of 6.3 in the presence of Baf has been reported by Yoshimori et al. (1991). The V-ATPase may not be the only factor responsible for pH homeostasis in late endosomes/lysosomes. Lysosomes maintain a mildly acidic pH after their isolation in the absence of ATP (Ohkuma et al., 1982). This acidification does not re-

quire an active influx of protons, but can be abolished by cations such as K^+ and Na^+ (Moriyama et al., 1992). Like Baf, amines and proton ionophores also increase the lysosomal pH to 6.0–6.5 (Ohkuma and Poole, 1978). A Donnan-type equilibrium may also be involved in maintenance of an acidic lysosomal pH (Reijngoud and Tager, 1977; Moriyama et al., 1992). Thus, although we showed that sorting between endocytosed ^{125}I-MPR and ^{125}I-Tf occurred independently of an active V-ATPase, formally we cannot exclude the possibility that this sorting is pH dependent.

In summary, we have confirmed that in the presence of Baf, early endosomes in intact cells fail to acidify due to inhibition of the vacuolar proton pump. Under these conditions, Tf failed to dissociate from its receptor, resulting in the continuous recycling of the Tf/TfR complex. The data show that endocytic uptake, recycling to the plasma membrane, and transport to late endosomes continue, although at slightly reduced rates, after inhibition of the vacuolar proton pump. In contrast, transport from late endosomes to lysosomes was nearly completely blocked.

We are grateful to Brigitte Groothuis and Janice Griffith for technical assistance, and Tom van Rijn and René Scriwanek for their help with the figures. We would like to thank Dr. A. L. Schwartz for antiserum against TfR, and Dr. K. von Figura for the antisera against MPR and cathepsin D.

This work was supported by grants from the Foundation for Medical Research, MEDIGON, The Netherlands (900-053-061); the Royal Netherlands Academy of Arts and Sciences (to W. Stoorvogel); and the National Institutes of Health (DK27083 to F. R. Maxfield).

Received for publication 20 October 1994 and in revised form 24 April 1995.

References

Ajioka, R. S., and J. Kaplan. 1986. Intracellular pools of transferrin receptors result from constitutive internalization of unoccupied receptors. *Proc. Natl. Acad. Sci. USA.* 83:6445–6449.

Ajioka, R. S., and J. Kaplan. 1987. Characterization of endocytic compartments using the horseradish-peroxidase–diaminobenzidine density shift technique. *J. Cell Biol.* 104:77–85.

Basu, S. K., J. L. Goldstein, R. G. W. Anderson, and M. S. Brown. 1981. Monensin interrupts the recycling of low density lipoprotein receptors in human fibroblasts. *Cell.* 24:493–502.

Bénaroch, P., M. Yilla, G. Raposo, K. Ito, K. Miwa, H. J. Geuze, and H. L. Ploegh. 1995. How MHC class II molecules reach the endocytic pathway. *EMBO (Eur. Mol. Biol. Organ.) J.* 14:37–49.

Bowman, E. J., A. Siebers, and K. Altendorf. 1988. Bafilomycins: a class of inhibitors of membrane ATPases from microorganisms, animal cells, and plant cells. *Proc. Natl. Acad. Sci. USA.* 85:7972–7976.

Braulke, T., C. Gartung, A. Hasilik, and K. von Figura. 1987. Is movement of mannose 6-phosphate–specific receptor triggered by binding of lysosomal enzymes? *J. Cell. Biol.* 104:1735–1742.

Cain, C. C., D. M. Spie, and R. F. Murphy. 1989. Regulation of endocytic pH by the Na^+,K^+-ATPase in living cells. *Proc. Natl. Acad. Sci. USA.* 86:544–548.

Chapman, R. E., and S. Munro. 1994. Retrieval of TGN proteins from the cell surface requires endosomal acidification. *EMBO (Eur. Mol. Biol. Organ.) J.* 13:2305–2312.

Ciechanover, A., A. L. Schwartz. A. Dautry-Varsat, and H. F. Lodish. 1983. Kinetics of internalization and recycling of transferrin and the transferrin receptor in a human hepatoma cell line. Effect of lysosomotropic agents. *J. Biol. Chem.* 258:9681–9689.

Clague, M. J., S. Urbe, F. Aniento, and J. Gruenberg. 1994. Vacuolar ATPase activity is required for endosomal carrier vesicle formation. *J. Biol. Chem.* 269:21–24.

Courtoy, P. 1991. Dissection of endosomes. *In* Trafficking of Membrane Proteins. J. C. Steer and J. Harford, editors. Academic Press, Inc. New York. 103–156.

Dautry-Varsat, A., A. Ciechanover, and H. F. Lodish. 1983. pH and the recycling of transferrin during receptor mediated endocytosis. *Proc. Natl. Acad. Sci. USA.* 80:2258–2262.

Dunn, K., J. Park, C. Semrad, D. Gelman, T. Shevell, and T. McGraw. 1994. Regulation of endocytic trafficking and acidification are independent of the cystic fibrosis transmembrane regulator. *J. Biol. Chem.* 269:5336–5345.

Feng, Y., and M. Forgac. 1994. Inhibition of vacuolar H(+)-ATPase by disulfide bond formation between cysteine 254 and cysteine 532 in subunit A. *J. Biol. Chem.* 269:13224–13230.

Fuchs, R., S. Schmid, and I. Mellman. 1989. A possible role for Na^+,K^+-ATPase in regulating ATP-dependent endosome acidification. *Proc. Natl. Acad. Sci. USA.* 86:539–543.

Geuze, H. J., W. Stoorvogel, G. J. Strous, J. W. Slot, J. E. Bleekemolen, and I. Mellman. 1988. Sorting of mannose 6-phosphate receptors and lysosomal membrane proteins in endocytic vesicles. *J. Cell Biol.* 107:2491–2501.

Gluck, S. L. 1993. The vacuolar H^+-ATPases: versatile proton pumps participating in constitutive and specialized functions of eucaryotic cells. *Int. Rev. Cytol.* 137C:105–137.

Gonzalez-Noriega, A., J. H. Grubb, V. Talkad, and W. S. Sly. 1980. Chloroquine inhibits lysosomal enzyme pinocytosis and enhances lysosomal enzyme secretion by impairing receptor recycling. *J. Cell Biol.* 85:839–852.

Gruenberg, J., G. Griffiths, and K. E. Howell. 1989. Characterization of the early endosome and putative endocytic carrier vesicles in vivo and with an assay of vesicle fusion in vitro. *J. Cell Biol.* 108:1301–1316.

Hanada, H., Y. Moriyama, M. Maeda, and M. Futai. 1990. Kinetic studies of chromaffin granule H^+-ATPase and effects of Bafilomycin A1. *Biochem. Biophys. Res. Commun.* 170:873–878.

Harding, C. V., and H. J. Geuze. 1992. Class II MHC molecules are present in macrophage lysosomes and phagolysosomes that function in the phagocytic processing of listeria monocytogenes for presentation to T cells. *J. Cell Biol.* 119:531–542.

Hubbard, A. L., and Z. A. Cohn. 1972. The enzymatic iodination of the red cell membrane. *J. Cell Biol.* 55:390–405.

Johnson, L. S., K. W. Dunn, B. Pytowsky, and T. E. McGraw. 1993. Endosome acidification and receptor trafficking: bafilomycin A1 slows receptor exit by a mechanism involving the receptors internalization motif. *Mol. Biol. Cell.* 4: 1251–1266.

Kiess, W., G. D. Blickenstaff, M. M. Sklar, C. L. Thomas, S. P. Nissley, and G. G. Sahagian. 1988. Biochemical evidence that the type II insulin-like growth factor receptor is identical to the cation-independent mannose 6-phosphate receptor. *J. Biol. Chem.* 263:9339–9344.

Klausner, R. D., G. Ashwell, J. van Renswoude, J. B. Harford, and K. R. Bridges. 1983. Binding of apotransferrin to K562 cells: explanation of the transferrin cycle. *Proc. Natl. Acad. Sci. USA.* 80:2263–2266.

Klumperman, J., A. Hille, T. Veenendaal, V. Oorschot, W. Stoorvogel, K. von Figura, and H. J. Geuze. 1993. Differences in the endosomal distributions of the two mannose 6-phosphate receptors. *J. Cell Biol.* 121:997–1010.

Knowles, B. B., C. C. Howe, and D. P. Aden. 1980. Human hepatocellular cell lines secrete the major plasma proteins and hepatitis B surface antigen. *Science (Wash. DC).* 209:497–499.

Kornfeld, S., and I. Mellman. 1989. The biogenesis of lysosomes. *Annu. Rev. Cell Biol.* 5:483–525.

Maxfield, F. R., and K. W. Dunn. 1990. Studies of endocytosis using image intensification for fluorescence microscopy and digital image analysis. *In* Optical Microscopy for Biology. B. Herman and K. Jacobson, editors. Wiley-Liss, New York. 357–371.

Maxfield, F. R., and D. J. Yamashiro. 1991. Acidification of organelles and the intracellular sorting of proteins during endocytosis. *In* Intracellular Trafficking of Proteins. C. J. Steer and J. A. Hanover, editors. Cambridge University Press, Cambridge UK. 157–182.

Mellman, I., H. Plutner, and P. Ukkonen. 1984. Internalization and rapid recycling of macrophage Fc receptors tagged with monovalent antireceptor antibody: possible role of a prelysosomal compartment. *J. Cell Biol.* 98:1163–1169.

Mellman, I., R. Fuchs, and A. Helenius. 1986. Acidification of the endocytic and exocytic pathways. *Annu. Rev. Biochem.* 55:663–700.

Morgan, D. O., J. C. Edman, D. N. Standring, V. A. Fried, M. C. Smith, R. A. Roth, and W. J. Rutter. 1987. Insulin-like growth factor II receptor as a multifunctional binding protein. *Nature (Lond.).* 329:301–307.

Moriyama, Y., M. Maeda, and M. Futai. 1992. Involvement of a non-proton-pump factor (possibly Donnan-type equilibrium) in maintenance of an acidic pH in lysosomes. *FEBS Lett.* 302:18–20.

Myers, M., and M. Forgac. 1993. The coated vesicle vacuolar (H^+)ATPase associates with and is phosphorylated by the 50-kDa polypeptide of the clathrin assembly protein AP-2. *J. Biol. Chem.* 268:9184–9186.

Octave, J-N., Y-J. Schnieder, P. Hoffmann, A. Trouet, and R. R. Crichton. 1982. *Eur. J. Biochem.* 123:235–240.

Ohkuma, S., and B. Poole. 1978. Fluorescence probe measurement of the intralysosomal pH in living cells and the perturbation of pH by various agents. *Proc. Natl. Acad. Sci. USA.* 75:3327–3331.

Ohkuma, S., Y. Moriyama, and T. Takano. 1982. Identification and characterization of a proton pump on lysosomes by fluorescein isothiocyanate–dextran fluorescence. *Proc. Natl. Acad. Sci. USA.* 79:2758–2762.

Pfeffer, S. R. 1987. The endosomal concentration of a mannose 6-phosphate receptor is unchanged in the absence of ligand synthesis. *J. Cell Biol.* 105:229–234.

Reaves, B., and G. Banting. 1994. Vacuolar ATPase inactivation blocks recycling to the trans-Golgi network from the plasma membrane. *FEBS Lett.* 345:61–66.

Reijngoud, D. J., and J. M. Tager. 1977. The permeability properties of the lysosomal membrane. *Biochim. Biophys. Acta.* 472:419–449.

Romanek, R., R. Sargeant, M. R. Paquet, S. Gluck, A. Klip, and S. Grinstein. 1993. Chloroquine inhibits glucose-transporter recruitment induced by insulin in rat adipocytes independently of its action on endomembrane pH. *Biochem. J.* 296:321–327.

Rijnboutt, S. R., W. Stoorvogel, G. J. Geuze, and G. J. Strous. 1992. Identification of subcellular compartments involved in biosynthetic processing of cathepsin D. *J. Biol. Chem.* 267:15665–15672.

Sahagian, G. G., J. Distler, and G. W. Jourdian. 1981. Characterization of a membrane-associated receptor from bovine liver that binds phosphomannosyl residues of bovine testicular β-galactosidase. *Proc. Natl. Acad. Sci. USA.* 78:4289–4293.

Schwartz, A. L., and D. Rup. 1983. Biosynthesis of the human asialoglycoprotein receptor. *J. Biol. Chem.* 258:11249–11255.

Schwartz, A. L., A. Bolognesi, and S. E. Fridovich. 1984. Recycling of the asialoglycoprotein receptor and the effect of lysosomotropic amines in hepatoma cells. *J. Cell Biol.* 98:732–738.

Slot, J. W., H. J. Geuze, S. Gigengack, G. E. Lienhard, and D. E. James. 1991. Immuno-localization of the insulin regulatable glucose transporter in brown adipose tissue of rat. *J. Cell Biol.* 113:123–135.

Stein, B. S., and H. H. Sussman. 1986. Demonstration of two distinct transferrin receptor recycling pathways and transferrin-independent receptor internalization in K562 cells. *J. Biol. Chem.* 261:10319–10331.

Stoorvogel, W., H. J. Geuze, and G. J. Strous. 1987. Sorting of endocytosed transferrin and asialoglycoprotein occurs immediately after internalization in HepG2 cells. *J. Cell. Biol.* 104:1261–1268.

Stoorvogel, W., H. J. Geuze, J. M. Griffith, and G. J. Strous. 1988. The pathways of endocytosed transferrin and secretory protein are connected in the *trans*-Golgi reticulum. *J. Cell Biol.* 106:1821–1829.

Stoorvogel, W., H. J. Geuze, J. M. Griffith, A. L. Schwartz, and G. J. Strous. 1989. Relations between the intracellular pathways of the receptors for transferrin, asialoglycoprotein, and mannose-6-phosphate in human hepatoma cells. *J. Cell Biol.* 108:2137–2148.

Stoorvogel, W., A. L. Schwartz, G. J. Strous, and R. J. Fallon. 1991*a*. A pool of intracellular phosphorylated asialoglycoprotein receptors which is not involved in endocytosis. *J. Biol. Chem.* 266:5438–5444.

Stoorvogel, W., G. J. Strous., H. J. Geuze, V. Oorschot, and A. L. Schwartz. 1991*b*. Late endosomes derive from early endosomes by maturation. *Cell.* 65:417–427.

Strous, G. J., A. Du Maine, J. E. Zijderhand-Bleekemolen, J. W. Slot, and A. L. Schwartz. 1985. Effect of lysosomotropic amines on the secretory pathway and on the recycling of the asialoglycoprotein receptor in human hepatoma cells. *J. Cell Biol.* 101:531–539.

Strous, G. J., P. van Kerkhof, G. van Meer, S. Rijnboutt, and W. Stoorvogel. 1993. Differential effects of brefeldin A on transport of secretory and lysosomal proteins. *J. Biol. Chem.* 268:2341–2347.

Tietze, C., P. Schlesinger, and P. Stahl. 1982. Mannose-specific endocytosis receptor of alveolar macrophages: demonstration of two functionally distinct intracellular pools of receptor and their roles in receptor recycling. *J. Cell Biol.* 92:417–424.

Tycko, B., C. H. Keith, and F. R. Maxfield. 1983. Rapid acidification of endocytic vesicles containing asialoglycoprotein in cells of a human hepatoma line. *J. Cell Biol.* 97:1762–1776.

Ukkonen, P., V. Lewis, M. Marsh, A. Helenius, and I. Mellman. 1986. Transport of macrophage Fc receptors and Fc receptor–bound ligands to lysosomes. *J. Exp. Med.* 163:952–971.

Umata, T., Y. Moriyama, M. Futai, and E. Mekada. 1990. The cytotoxic action of diphtheria toxin and its degradation in intact Vero cells are inhibited by bafilomycin A1, a specific inhibitor of vacuolar-type H^+-ATPase. *J. Biol. Chem.* 265:21940–21945.

Van Deurs, B., O. W. Petersen, S. Olsnes, and K. Sandvig. 1989. The ways of endocytosis. *Int. Rev. Cytol.* 117:131–177.

von Figura, K., V. Gieselmann, and A. Hasilik. 1984. Antibody to mannose 6-phosphate specific receptor induces receptor deficiency in human fibroblasts. *EMBO (Eur. Mol. Biol. Organ.) J.* 3:1281–1286.

Werner, G., H. Hagenmaier, H. Drautz, A. Baumgartner, and H. Zähner. 1984. Bafilomycins, a new group of macrolide antibiotics. Production, isolation, chemical structure, and biological activity. *J. Antibiot. (Tokyo).* 37:110–117.

Willingham, M. C., I. H. Pastan, and G. G. Sahagian. 1983. Ultrastructural immunocytochemical localization of the phosphomannosyl receptor in Chinese hamster ovary (CHO) cells. *J. Histochem. Cytochem.* 31:1–11.

Xie, X-S., B. P. Crider, Y-M. Ma, and D. K. Stone. 1994. Role of a 50–57-kDa polypeptide heterodimer in the function of the clathrin-coated vesicle proton pump. *J. Biol. Chem.* 269:25809–25815.

Yamashiro, D., B. Tycko, S. Fluss, and F. Maxfield. 1984. Segregation of Tf to a mildly acidic (pH 6.5) compartment in the recycling pathway. *Cell.* 37:789–800.

Yoshimori, T., A. Yamamoto, Y. Moriyama, M. Futai, and Y. Tashiro. 1991. Bafilomycin A1, a specific inhibitor of vacuolar-type H^+-ATPase, inhibits acidification and protein degradation in lysosomes of cultured cells. *J. Biol. Chem.* 266:17707–17712.

Zhang, J., Y. Feng, and M. Forgac. 1994. Proton conduction and bafilomycin binding by the V_0 domain of the coated vesicle V-ATPase. *J. Biol. Chem.* 269:23518–23523.

Zhang, K., Z.-Q. Wang, and S. Gluck. 1992*a*. Identification and partial purification of a cytosolic activator of vacuolar H^+-ATPases from mammalian kidney. *J. Biol. Chem.* 267:9701–9705.

Zhang, K., Z.-Q. Wang, and S. Gluck. 1992*b*. A cytosolic inhibitor of vacuolar H^+-ATPases from mammalian kidney. *J. Biol. Chem.* 267:14539–14542.

Zijderhand-Bleekemolen, J. E., A. L. Schwartz, J. W. Slot, G. J. Strous, and H. J. Geuze. 1987. Ligand– and weak base-induced redistribution of asialoglycoprotein receptors in hepatoma cells. *J. Cell Biol.* 104:1647–1654.